

Time-Resolved FRET Biosensor Based on Amine-Functionalized Lanthanide-Doped NaYF₄ Nanocrystals**

Datao Tu, Liqin Liu, Qiang Ju, Yongsheng Liu, Haomiao Zhu, Renfu Li, and Xueyuan Chen*

Recently, nanocrystals (NCs) doped with lanthanides (Ln³⁺) have come to the forefront of functional nanomaterials for a variety of biological applications due to their sharp f-f emission peaks, long photoluminescence (PL) lifetimes, and large Stokes shifts.^[1] Compared to traditional organic fluorophores and quantum dots (QDs) commonly used in bioimaging and biodetection, Ln³⁺-doped NCs show superior features such as high chemical stability, high resistance to photobleaching, and low toxicity.^[2] A significant application of Ln³⁺-doped NCs is the development of novel luminescent biosensors based on fluorescence resonance energy transfer (FRET), a nonradiative process characterized by energy transfer between an excited donor fluorophore (e.g., Ln³⁺-doped NC) and an acceptor fluorophore (e.g., organic dye) through long-range dipole-dipole interactions.^[3] The donor and acceptor fluorophores are linked in close proximity, typically less than a few nanometers, through bioconjugation.^[3b] This energy-transfer process can be detected by monitoring the PL emission spectra of acceptor and donor upon excitation of the donor. The change in PL emission intensity is sensitive to the concentration of target biomolecules introduced for bioconjugation between donor and acceptor.^[4] Unfortunately, for conventional FRET assays with steady-state detection mode, the sensitivity of fluorescence detection is severely compromised by autofluorescence interference, which limits practical application of the FRET technique involving UV-excited bioprobes such as organic dyes, Ln³⁺ chelates, and QDs.

To avoid autofluorescence and improve detection sensitivity, some novel FRET assay techniques have emerged. For instance, upconversion FRET (UC-FRET) assay has been

introduced as a good candidate for quantitative detection of biological samples, whereby UC phosphors are excited in the near-infrared (NIR) region to achieve visible emissions, so that no autofluorescence is produced from biocompounds.^[5] Time-resolved FRET (TR-FRET) employing the long-lived PL of lanthanide ions such as Tb³⁺ and Eu³⁺ is another effective strategy to completely eliminate the interference of scattered light and autofluorescence from cells and tissues, as previously proposed for molecular probes such as Ln³⁺ chelates.^[6] The PL lifetime of typical lanthanide complexes is on the order of a few milliseconds or longer,^[7] in sharp contrast to those of common organic dyes and biocompounds, which lie typically in the nanosecond range.^[4] In a TR-FRET analysis, energy transfer from the donors such as Ln³⁺ chelates will apparently lengthen the PL lifetime of acceptors such as organic dyes, which are intrinsically short-lived,^[6c] due to slow population of the acceptor excited state from the long-lived Ln³⁺ excited state. On the basis of this principle, the TR-FRET signal can be measured free of the interference of short-lived background by setting appropriate delay time and gate time (Figure 1). This method offers a signal with

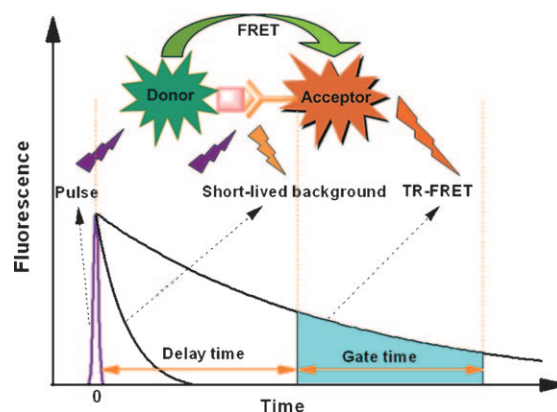


Figure 1. The principle of luminescent biodetection based on the TR-FRET technique.

remarkably high signal-to-noise ratio in luminescent biodetection as compared to conventional FRET. Thus far, molecular probes based on Ln³⁺ chelates have been developed as TR-FRET bioprobes in various immunoassays because of their long PL lifetimes, often longer than 1 ms, and large Stokes shifts (> 200 nm). However, most Ln³⁺ chelates are susceptible to photobleaching under intense and continuous excitation.^[8] Herein we present the first demonstration of TR-FRET biosensing based on amine-functionalized Ln³⁺-doped NCs. As opposed to Ln³⁺ chelates,

[*] D. T. Tu, Dr. L. Q. Liu, Dr. Q. Ju, Dr. Y. S. Liu, Dr. H. M. Zhu, R. F. Li, Prof. X. Y. Chen

Key Laboratory of Optoelectronic Materials Chemistry and Physics
Fujian Institute of Research on the Structure of Matter
Chinese Academy of Sciences, Fuzhou, Fujian 350002 (China)
Fax: (+86)591-8764-2575
and
State Key Laboratory of Structural Chemistry
Fuzhou, Fujian 350002 (China)
E-mail: xchen@fjirsm.ac.cn

[**] This work is supported by the Hundred Talent Program of the Chinese Academy of Sciences (CAS), Knowledge Innovation Program of CAS for Key Topics (No. KJCX2-YW-358), the NSFC (Nos. 10974200 and 51002151), the 973 and 863 programs of MOST (Nos. 2007CB936703 and 2009AA03Z430), and the NSF of Fujian Province for Distinguished Young Scholars (Nos. 2009J05138, 2009J06030 and 2010J05126).

Supporting information for this article (detailed experimental procedures) is available on the WWW under <http://dx.doi.org/10.1002/anie.201100303>.

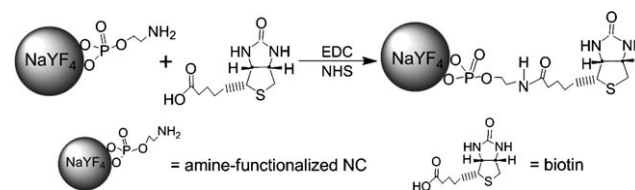
these NCs have rigid crystal lattices and high photostability against continuous excitation and repetitive assays. By using our model system, we show that trace amounts of biomolecules such as avidin can be readily detected down to about 5 nm.

Currently, NaYF₄ is recognized as one of the most efficient host for both UC and downconversion PL because of its low lattice phonon energy (< 400 cm⁻¹).^[9] Considerable efforts have been devoted to controlled synthesis and optical characterization of Ln³⁺-doped NaYF₄ NCs.^[10] However, most of these NCs were prepared in hydrophobic organic solvents and are not water-soluble due to the lack of hydrophilic functional groups on their surfaces. Typically, additional surface-modification steps are required to create a hydrophilic surface bearing appropriate functional groups (e.g., COOH, NH₂, or SH) for further conjugation of biomolecules.^[11] The complicated and time-consuming post-treatment procedures may affect the morphology and PL intensity of NCs, and this is unfavorable for potential applications of Ln³⁺-based NaYF₄ NCs. In this regard, we developed a direct one-step solvothermal route to prepare amine-functionalized NaYF₄:Ce/Tb NCs with 2-aminoethyl dihydrogenphosphate (AEP) as surfactant that anchors on the surface of the particles and provides a platform for subsequent conjugation with biomolecules.

In a typical experiment, amine-functionalized NaYF₄:Ce/Tb NCs were synthesized by a facile modified one-step solvothermal method with AEP as capping agent to control the growth of NCs and to render them water-soluble and surface-functionalized.^[12] Transmission electron microscopy (TEM) images showed that the as-prepared NCs are roughly spherical with a size distribution ranging from 20 to 40 nm (Figure S1, Supporting Information). Clear lattice fringes observed in the high-resolution TEM (HRTEM) image (Figure S1) reveal high crystallinity of the NCs. The distance of 0.31 nm between adjacent lattice fringes is consistent with the *d* spacing for the (111) plane of cubic NaYF₄. The powder XRD pattern of the NCs can be exclusively indexed to pure cubic phase of NaYF₄ (JCPDS No. 77-2042) without any other impurities (Figure S1). Compositional analysis by energy-dispersive X-ray spectroscopy (EDS) indicated successful incorporation of Ce³⁺ and Tb³⁺ ions into the NaYF₄ lattice (Figure S1). In addition, identification of P and C by EDS verifies the presence of AEP on the surface of the NCs (Figure S2). The major stages of weight loss for both the NCs and pure AEP by thermogravimetric analysis (TGA) are nearly identical (Figure S3), which provides additional evidence for capping of the NCs by AEP.

The presence of AEP as a surfactant overlayer on the NCs enables them to be amine-functionalized and readily dispersed in water. The NC solution remains stable at room temperature for more than one month and no precipitate or aggregate was observed. The surface functional groups of NCs can be identified by FTIR spectroscopy (Figure S4). A strong IR band centered at 1635 cm⁻¹ was observed for the as-prepared NaYF₄ NCs, which is attributed to the N–H stretching mode of the amino groups of AEP. The free amino groups on the surface of NCs allow further conjugation with biomolecules such as biotin, by following the well-

established EDC/NHS protocol (Scheme 1),^[5a] in which biotin is covalently bound to an amine-functionalized NC through its carboxy group by using the cross-linking reagent



Scheme 1. Biotinylation of amine-enriched NCs. EDC = 1-ethyl-3-(3-dimethylaminopropyl) carbodiimide, NHS = *N*-hydroxysuccinimide.

EDC and NHS in phosphate-buffered saline (PBS) solution at room temperature. In contrast to that of the as-prepared NCs, the FTIR spectrum of biotinylated NCs (Figure S4) displays a new peak at 1688 cm⁻¹, ascribed to the stretching vibration of an amide bond. Moreover, a high-energy vibrational band centered at 3312 cm⁻¹ and two bands centered at 1204 and 1142 cm⁻¹ were exclusively observed in biotinylated NCs, and are assigned to the N–H and C–N stretching vibrations of biotin, respectively. These findings show unambiguously successful attachment of biotin to the surface of NCs, which enables specific binding with proteins such as avidin for versatile bioapplications.

The optical properties of the as-prepared and biotinylated NCs in aqueous solutions with the same mass concentration were systematically investigated at room temperature (Figure 2). Upon excitation at 290 nm, which corresponds to the 4f→5d transition of Ce³⁺, both colloidal solutions exhibited two sets of emissions in the UV and visible regions. The relatively weak and broad UV emission band from 300 to 400 nm is associated with the 5d→4f transition of Ce³⁺, and the intense and sharp emission bands centered at 489, 542, 585, and 623 nm are assigned to ⁵D₄→⁷F_{*J*} (*J* = 6, 5, 4, 3) of Tb³⁺, which suggests that the intense emissions from Tb³⁺ are realized via sensitization of Ce³⁺.^[13] As shown in the insets of Figure 2, the as-prepared NC solution exhibits strong green

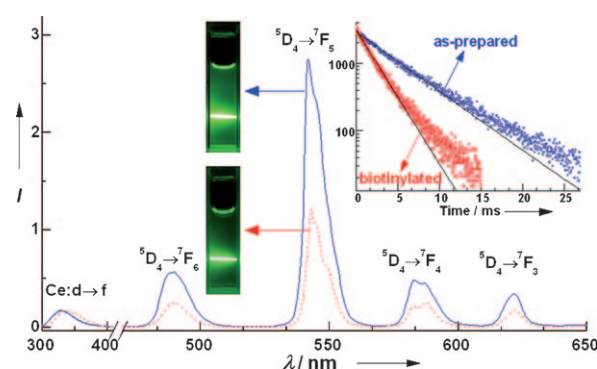
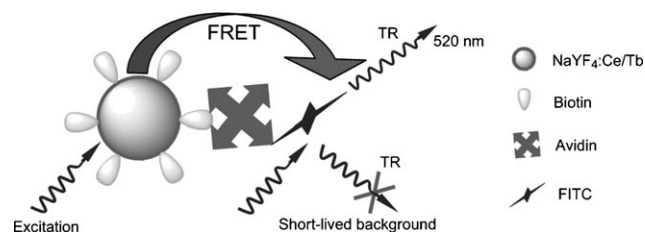


Figure 2. Emission spectra for the as-prepared (solid line) and biotinylated (dashed line) NC solutions. The inset on the upper right shows the corresponding PL decays from ⁵D₄ of Tb³⁺. The insets on the left show corresponding PL photographs, taken with an exposure time of 1.0 s, when both samples were irradiated at 290 nm with a 1 mW Ti:sapphire third-harmonic generation (THG) laser.

emission, whereas the PL intensity of the biotinylated NC solution is somewhat lower. The essentially unaltered PL intensities of both solutions after continuous irradiation by UV lamp (2–4% decrease over 2 h; Figure S5) indicate high photostability of the NC solutions. The quantum yield (QY), defined as the ratio of the number of emitted photons to the number of absorbed photons,^[14] was determined to be 56.4 and 28.9% for the as-prepared NCs and their biotinylated counterparts, respectively. To evaluate potential applications in TR-FRET detection, we measured the PL lifetimes of the 5D_4 state of Tb^{3+} ion in both solutions under excitation at 290 nm by monitoring the characteristic emission at 542 nm. Both decay curves (inset in Figure 2) fit well to a single-exponential function, and the PL lifetimes were determined to be 4.76 and 2.21 ms for the as-prepared and biotinylated NC solutions, respectively. Evidently, the PL lifetime of Tb^{3+} in the biotinylated NC solution is noticeably shorter than that of the as-prepared counterpart. Owing to its long PL lifetime, the luminescence of Tb^{3+} is expected to be easily distinguishable from the undesired short-lived background fluorescence. The intense emission, high quantum efficiency, and long PL lifetime for both solutions are closely related to the large energy gap between 5D_4 and its next lower lying 7F_J ($J = 3, 4, 5, 6$) states of Tb^{3+} .^[15] The weaker PL intensity, lower quantum yield, and shorter PL lifetime of NCs after biotinylation may be due to nonradiative-relaxation-induced PL quenching associated with the surface high-energy vibronic groups^[16] (N–H and C–N) of biotin, as already revealed in the FTIR spectra.

To demonstrate the use of biotinylated NCs as biosensors in quantitative luminescence bioassays, they were used for detection of traces of avidin, in view of the high affinity between avidin and biotin ($K_a = 10^{15} M^{-1}$).^[17] The principle of TR-FRET detection of avidin by employing biotinylated NCs as energy donor and fluorescein isothiocyanate (FITC)-labeled avidin as energy acceptor is illustrated in Scheme 2.



Scheme 2. TR-FRET detection of avidin by employing biotinylated NCs as donor and FITC as acceptor.

Excitation of biotinylated NCs triggers energy transfer to FITC within a given proximity through specific binding between biotin and avidin, and results in emission from FITC at its characteristic wavelength. Here FITC was selected as an energy acceptor to couple with the NC, because it has a broad excitation peak at 490 nm that matches well with the $^5D_4 \rightarrow ^7F_6$ emission band of Tb^{3+} centered at 489 nm (Figure 3a). More importantly, the short-lived broad-band emission of FITC arising from direct UV excitation, which partially overlaps with that of Tb^{3+} , can be distinguished easily from the long-

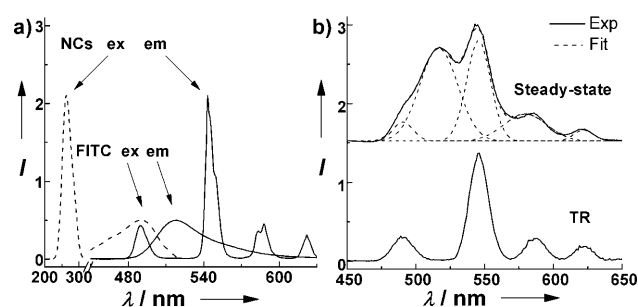


Figure 3. a) Excitation (dashed line) and emission (solid line) spectra of biotinylated NCs; excitation (dashed line) and emission (solid line) spectra of FITC. b) Steady-state and TR-PL (delay time = 100 μs , gate time = 1 ms) spectra of a mixture of 0.1 mM biotinylated NCs and 1 μM FITC under excitation at 290 nm. In steady-state detection, PL emissions of FITC and Tb^{3+} can be separated from the spectral deconvolution. The spectrum within 450–650 nm was best-fitted and deconvoluted to five Gaussian curves with peaks centered at 489, 520, 542, 585, and 623 nm.

lived emission of Tb^{3+} or apparently long lived emission of FITC due to FRET by employing TR detection. For example, the steady-state PL spectrum of a mixture of biotinylated NCs (0.1 mM) and FITC (1 μM) was dominated by the emission of FITC, and the emission bands from Tb^{3+} were hardly observed due to interference from the FITC emission band (Figure 3b). In sharp contrast, only intense emission lines originating from Tb^{3+} were detected in the TR PL spectra when the delay time and gate time were set to 100 μs and 1 ms, respectively (Figure 3b). These results verify that the TR technique, by utilizing the long-lived luminescence of emitters, is particularly effective in removing undesired short-lived background fluorescence. The proposed TR-FRET detection based on Ln^{3+} -doped inorganic NCs brings together the advantage of very low background of the TR technique and the convenience of homogeneous assay from FRET.

The process for a homogeneous TR-FRET assay is as follows: different concentrations of avidin labeled with FITC were added to the microplate wells, followed by addition to each well of the same amount of biotinylated NCs dispersed in buffered solution (pH 7.2). The plate was incubated at room temperature for 30 min and then subjected to TR-FRET measurements on a Synergy 4 microplate reader (BioTeK) without any other post-treatment such as centrifugation and washing, which are typical of heterogeneous assays. As shown in Figure 4a, upon excitation of NCs at 290 nm, the TR-FRET signal represented by a broad emission band of FITC centered at 520 nm (hereafter referred to as FITC₅₂₀) is gradually enhanced at the expense of the $^5D_4 \rightarrow ^7F_6$ PL emission band of Tb^{3+} centered at 489 nm (hereafter referred to as Tb₄₈₉) with increasing amount of FITC-labeled avidin. The concentration of avidin can be quantified by determining the integrated PL intensity ratio FITC₅₂₀/Tb₄₈₉ from the observed TR-FRET spectra (Figure S6). As shown in the measured calibration curve (Figure 4b), the TR-FRET signal of FITC₅₂₀/Tb₄₈₉ increases steadily until the avidin concentration to be detected approaches a value higher than 400 nM. For comparison, nonbinding control experiments were performed by employing the as-prepared NCs instead of

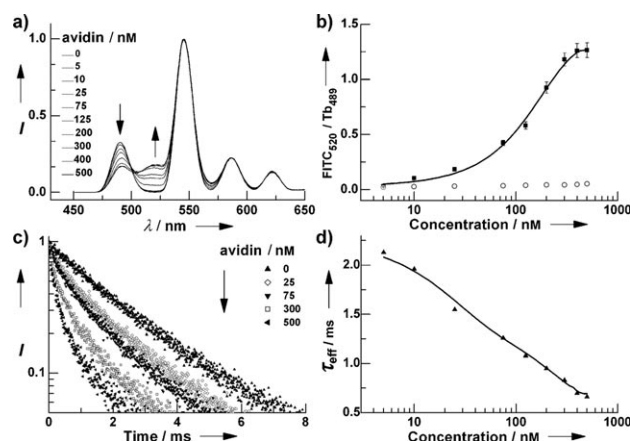


Figure 4. a) TR-FRET spectra of bioassay experiments at different concentrations of avidin. The delay and gate times were set to 100 μ s and 1 ms, respectively. The spectra were normalized to unity at the maximum emission peak at 542 nm and each data point represents the average of triplicate measurements. b) Calibration curve of TR-FRET detection for the integrated PL intensity ratio $\text{FITC}_{520}/\text{Tb}_{489}$ versus the concentration of avidin. The filled symbols indicate bioassay experiments in which FITC is FRET-sensitized by NCs through the avidin–biotin interaction. The open symbols show the control experiments with FITC-labeled avidin and amine-enriched NCs, for which no binding and hence no FRET occurs. c) Decay curves of $^5\text{D}_4$ of Tb^{3+} at different concentrations of avidin. d) Effective PL lifetime of $^5\text{D}_4$ of Tb^{3+} as a function of avidin concentration.

the biotinylated NCs as bioprobes under otherwise identical conditions. The specific interaction between biotin and avidin plays a key role to ensure proximity between the acceptor and the donor. Non-biotinylated NCs and FITC are far apart in solution, and thus no FRET occurred in the control experiments (Figure S7). As a result, the TR-FRET signals observed in the control experiments remain very low for avidin concentrations from a few nM to 400 nM (Figure 4b). The limit of detection (LOD), defined as the concentration that corresponds to three times the standard deviation above the signal measured in the control experiment,^[6c] is 4.8 nM. So far, no LOD of TR-FRET biodetection based on Ln^{3+} -doped inorganic NCs is available in the literature. However, our LOD is comparable to previous results based on UC-FRET employing $\text{Y}_2\text{O}_3\text{:Er/Yb}$ phosphors as donor and fluorescent phycobiliprotein as acceptor (0.7–9.0 nM).^[18]

The resonance energy transfer process is further confirmed by PL decay measurements. The FRET-induced PL decay of FITC in the tail (>0.05 ms) was observed to be markedly prolonged to hundreds of microseconds with increasing concentration of FITC-labeled avidin because of the slow population of its excited state from the long-lived Tb^{3+} excited state (Figure S8). Consistently, the decay curve of the $^5\text{D}_4$ state of Tb^{3+} involved in FRET deviated more seriously from single-exponential form with increasing avidin concentration (Figure 4c). This is because the Tb^{3+} ions located at or near the surface of the NCs play a more important role than those inside the NCs in the FRET process. Similar PL decays of the Tb^{3+} donor in LaPO_4 NCs were observed by Gu et al.^[3a] Note that Gu et al. reported only the decrease in PL lifetime of the donor to characterize

the FRET process, because a quencher-like Au acceptor was used, and no demonstration of TR-FRET biodetection was achieved. By contrast, PL lifetime lengthening of the acceptor and lifetime shortening of the donor were consistently observed in our work, and unambiguously support the occurrence of FRET. An effective PL lifetime τ_{eff} , defined as $(1/I_0) \int I(t) dt$, is adopted to characterize the nonexponential PL decays of Tb^{3+} .^[19] As shown in Figure 4d, the τ_{eff} value is significantly reduced from 2.2 to 0.7 ms with increasing concentration from 5 to 500 nM and tends to be constant at higher concentration above 400 nM. The evolution of τ_{eff} as a function of avidin concentration resembles the calibration curve of TR-FRET ($\text{FITC}_{520}/\text{Tb}_{489}$), as revealed from the similarity between Figure 4b and d. Therefore, the PL lifetime of the energy donor, which is hardly affected by environmental factors such as re-absorption and the concentration of NCs, may provide another important parameter other than the PL intensity to measure the energy-transfer efficiency in TR-FRET bioassays.

In summary, we have synthesized water-soluble, amine-functionalized cubic $\text{NaYF}_4\text{:Ce/Tb}$ NCs by a modified one-step solvothermal route by employing AEP as surfactant and capping agent. The NC solution exhibited intense PL emission and long PL lifetime (a few milliseconds), which thus allows one to completely eliminate the interference of short-lived background fluorescence by means of TR detection. The biotinylated NCs were used as efficient TR-FRET probes to detect trace amounts of avidin in a typical avidin–biotin model system with a detection limit of about 5 nM. As a new type of TR-FRET bioprobe, Ln^{3+} -based inorganic NCs have desirable advantages such as low cost, excellent water dispersibility and photostability, absence of autofluorescence, and low detection limit, and thus may have great potential for versatile applications in time-resolved biodetection and bio-imaging.

Received: January 13, 2011

Revised: February 28, 2011

Published online: May 24, 2011

Keywords: biosensors · FRET · lanthanides · luminescence · nanoparticles

- [1] a) F. Auzel, *Chem. Rev.* **2004**, *104*, 139–173; b) H. S. Mader, P. Kele, S. M. Saleh, O. S. Wolfbeis, *Curr. Opin. Chem. Biol.* **2010**, *14*, 582–596; c) Q. Ju, W. Q. Luo, Y. S. Liu, H. M. Zhu, R. F. Li, X. Y. Chen, *Nanoscale* **2010**, *2*, 1208–1212; d) R. Kumar, M. Nyk, T. Y. Ohulchanskyy, C. A. Flask, P. N. Prasad, *Adv. Funct. Mater.* **2009**, *19*, 853–859; e) F. Wang, J. Wang, X. Liu, *Angew. Chem.* **2010**, *122*, 7618–7622; *Angew. Chem. Int. Ed.* **2010**, *49*, 7456–7460; f) F. Wang, Y. Han, C. S. Lim, Y. Lu, J. Wang, J. Xu, H. Chen, C. Zhang, M. Hong, X. Liu, *Nature* **2010**, *463*, 1061–1065; g) P. Ptacek, H. Schäfer, K. Kömpe, M. Haase, *Adv. Funct. Mater.* **2007**, *17*, 3843–3848; h) F. Wang, X. Liu, *Chem. Soc. Rev.* **2009**, *38*, 976–989; i) P. Rahman, M. Green, *Nanoscale* **2009**, *1*, 214–224; j) C. Jiang, F. Wang, N. Wu, X. Liu, *Adv. Mater.* **2008**, *20*, 4826–4829; k) H. Schäfer, M. Haase, *Angew. Chem.* **2011**, DOI: 10.1002/ange.201005159; *Angew. Chem. Int. Ed.* **2011**, DOI: 10.1002/anie.201005159.

- [2] a) F. Vetrone, R. Naccache, V. Mahalingam, C. G. Morgan, J. A. Capobianco, *Adv. Funct. Mater.* **2009**, *19*, 2924–2929; b) F. Vetrone, R. Naccache, A. J. de La Fuente, F. Sanz-Rodríguez, A. Blazquez-Castro, E. M. Rodríguez, D. Jaque, J. G. Solé, J. A. Capobianco, *Nanoscale* **2010**, *2*, 495–498; c) M. Nyk, R. Kumar, T. Y. Ohulchanskyy, E. J. Bergey, P. N. Prasad, *Nano. Lett.* **2008**, *8*, 3834–3838; d) F. Wang, D. Banerjee, Y. Liu, X. Chen, X. Liu, *Analyst* **2010**, *135*, 1839–1854; e) J. Wang, F. Wang, J. Xu, Y. Wang, Y. Liu, X. Chen, H. Chen, X. Liu, *C. R. Chim.* **2010**, *13*, 731–736; f) H. Schäfer, P. Ptacek, O. Zerzouf, M. Haase, *Adv. Funct. Mater.* **2008**, *18*, 2913–2918.
- [3] a) J. Q. Gu, J. Shen, L. D. Sun, C. H. Yan, *J. Phys. Chem. C* **2008**, *112*, 6589–6593; b) S. Hu, H. Yang, R. X. Cai, Z. S. Liu, X. L. Yang, *Talanta* **2009**, *80*, 454–458.
- [4] L. Wang, B. B. Qian, H. Q. Chen, Y. Liu, A. Liang, *Chem. Lett.* **2008**, *37*, 402–403.
- [5] a) L. Y. Wang, R. X. Yan, Z. Y. Hao, L. Wang, J. H. Zeng, H. Bao, X. Wang, Q. Peng, Y. D. Li, *Angew. Chem.* **2005**, *117*, 6208–6211; *Angew. Chem. Int. Ed.* **2005**, *44*, 6054–6057; b) M. Wang, W. Hou, C. C. Mi, W. X. Wang, Z. R. Xu, H. H. Teng, C. B. Mao, S. K. Xu, *Anal. Chem.* **2009**, *81*, 8783–8789; c) S. Jiang, Y. Zhang, *Langmuir* **2010**, *26*, 6689–6694; d) T. Rantanen, M. L. Järvenpää, J. Vuojola, R. Arppe, K. Kuningas, T. Soukka, *Analyst* **2009**, *134*, 1713–1716; e) A. Bednarkiewicz, M. Nyk, M. Samoc, W. Strek, *J. Phys. Chem. C* **2010**, *114*, 17535–17541.
- [6] a) H. Rajapakse, D. Reddy, S. Mohandessi, N. Butlin, L. Miller, *Angew. Chem.* **2009**, *121*, 5090–5092; *Angew. Chem. Int. Ed.* **2009**, *48*, 4990–4992; b) S. H. Kim, J. R. Gunther, J. A. Katzenellenbogen, *J. Am. Chem. Soc.* **2010**, *132*, 4685–4692; c) D. Geißler, L. J. Charbonniere, R. F. Ziessel, N. G. Butlin, H. G. Löhmansröben, N. Hildebrandt, *Angew. Chem.* **2010**, *122*, 1438–1443; *Angew. Chem. Int. Ed.* **2010**, *49*, 1396–1401.
- [7] K. Hanaoka, K. Kikuchi, S. Kobayashi, T. Nagano, *J. Am. Chem. Soc.* **2007**, *129*, 13502–13509.
- [8] a) M. Q. Tan, Z. Q. Ye, G. L. Wang, J. L. Yuan, *Chem. Mater.* **2004**, *16*, 2494–2498; b) Z. Q. Ye, M. Q. Tan, G. L. Wang, J. L. Yuan, *Anal. Chem.* **2004**, *76*, 513–518; c) H. Zhang, Y. Xu, W. Yang, Q. G. Li, *Chem. Mater.* **2007**, *19*, 5875–5881.
- [9] a) D. K. Ma, D. P. Yang, J. L. Jiang, P. Cai, S. M. Huang, *CrystEngComm* **2010**, *12*, 1650–1658; b) F. Wang, J. Wang, J. Xu, X. Xue, H. Chen, X. Liu, *Spectrosc. Lett.* **2010**, *43*, 400–405.
- [10] a) G. Y. Chen, T. Y. Ohulchanskyy, R. Kumar, H. Agren, P. N. Prasad, *ACS Nano* **2010**, *4*, 3163–3168; b) Z. Q. Li, Y. Zhang, *Angew. Chem.* **2006**, *118*, 7896–7899; *Angew. Chem. Int. Ed.* **2006**, *45*, 7732–7735; c) Z. Q. Li, Y. Zhang, S. Jiang, *Adv. Mater.* **2008**, *20*, 4765–4769; d) C. Yan, A. Dadvand, F. Rosei, D. F. Perepichka, *J. Am. Chem. Soc.* **2010**, *132*, 8868–8869; e) H. Schäfer, P. Ptacek, K. Kömpe, M. Haase, *Chem. Mater.* **2007**, *19*, 1396–1400; f) H. Schäfer, P. Ptacek, H. Eickmeier, M. Haase, *Adv. Funct. Mater.* **2009**, *19*, 3091–3097; g) G. S. Yi, G. M. Chow, *Adv. Funct. Mater.* **2006**, *16*, 2324–2329.
- [11] a) Z. G. Chen, H. L. Chen, H. Hu, M. X. Yu, F. Y. Li, Q. Zhang, Z. G. Zhou, T. Yi, C. H. Huang, *J. Am. Chem. Soc.* **2008**, *130*, 3023–3029; b) C. Liu, H. Wang, X. Li, D. Chen, *J. Mater. Chem.* **2009**, *19*, 3546–3553.
- [12] C. H. Dong, M. Raudsepp, F. C. J. M. van Veggel, *J. Phys. Chem. C* **2009**, *113*, 472–478.
- [13] W. H. Di, X. X. Zhao, Z. G. Nie, X. J. Wang, S. Z. Lu, H. F. Zhao, X. G. Ren, *J. Lumin.* **2010**, *130*, 728–732.
- [14] J. C. G. Bünzli, *Chem. Rev.* **2010**, *110*, 2729–2755.
- [15] Q. A. Lü, Y. J. Wu, L. R. Ding, G. M. Zu, A. H. Li, Y. M. Zhao, H. Cui, *J. Alloys Compd.* **2010**, *496*, 488–493.
- [16] Y. B. Li, Z. Sun, L. Ma, X. Zhang, M. Z. Yao, A. G. Joly, Z. L. Liu, W. Chen, *Nanotechnology* **2010**, *21*, 125604–125610.
- [17] a) H. J. Choi, N. H. Kim, B. H. Chung, G. H. Seong, *Anal. Biochem.* **2005**, *347*, 60–66; b) X. Zeng, Y. X. Sun, W. Qu, X. Z. Zhang, R. X. Zhuo, *Biomaterials* **2010**, *31*, 4771–4780.
- [18] K. Kuningas, T. Rantanen, T. Ukonaho, T. Lövgren, T. Soukka, *Anal. Chem.* **2005**, *77*, 7348–7355.
- [19] J. T. Kong, H. M. Zhu, R. F. Li, W. Q. Luo, X. Y. Chen, *Opt. Lett.* **2009**, *34*, 1873–1875.